Atomic and Close-to-atomic Scale Fabrication of Large-scale Solid-state Nanopore Array

Jufan Zhang[1,#], Hongshuai Liu[1], Boyuan Pang[1], Fengzhou Fang[1]

1 Centre of Micro/Nano Manufacturing Technology (MNMT-Dublin), School of Mechanical and Materials Engineering, University College Dublin, Dublin, D04V1W8, Ireland

Corresponding Author / Email: Jufan.zhang@ucd.ie, TEL: +353-1-7161733

KEYWORDS: Nanopore, Micropore, Manufacturing, ACSM, Nanotechnology

Nanopore has obtained great success in DNA sequencing. However, manufacturing solid-state nanopores in a large scale is still a challenge, limiting its uptake in industry. In this article, a hybrid manufacturing method is validated in fabricating a large quantity of solid-state nanopores simultaneously. Experiments have evidenced nanopore chip size over 100 mm^2 accommodating over 2.6 billion solid-state nanopores, with pore size down to 20-70 nm when maintaining a good uniformity, and minimum nanopore film thickness reaching 4 nm. Simulation revealed a directed atomic migration mechanism for regulating the 3D geometry of nanopores, and proved an unprecedented inhomogeneous pore channel variation phenomenon, as well as observed the closure of nanopores. The whole fabrication cycle is less than 3 hours with a high cost-effectiveness for mass production and industrial applications.

1. Introduction

Nanopore is a tiny hole of 1~100 nm in size [1]. Biological nanopores have gained great commercial success in DNA sequencing, which provides new possibilities and extraordinary performance for studying particles at single molecule level. However, as existing large molecules, dimensions and structures of biological nanopores are predetermined by nature, with limited flexibility in tuning their properties. Compared with biological pores, solid-state nanopores formed in engineering materials can realize controllable size, shape, and physiochemical properties, with better robustness, duration, stability, lower requirements on preserve and utilization environment, and more compatible with scalable production techniques [2,3]. However, limited by manufacturing technologies, solid-state nanopores have not achieved wide commercialization successfully. Currently, most fabrication methods still create single nanopores at a time with low efficiency and high cost [4]. Thus, even though some research preliminarily demonstrated the superior performance of solid-state nanopore array over single nanopore sensor, only limited progress in the lab has been reported, such as using 4, 9 or 36 solid-state nanopores [5-7]. Some company tried to integrate hundreds of thousands of biological nanopores into a device to achieve high throughput, but considering each biological nanopore is a separate molecule working independently, rigid combination of single nanopores is not a cost-effective and sustainable way, resulting in a high cost that unaffordable for most users [8]. This realistically reflects the state-of-the-art and the dilemma in nanopore array fabrication. To date, successful manufacturing of large-scale (millions to billions of) solid-state nanopore array has not been reported.

This paper proposes an innovative hybrid manufacturing method for efficient and cost-effective fabrication of large-scale solid-state nanopore array chips. The method combines nano-template fabrication, film deposition, nanopore array forming, and 3-dimentional shaping of nanopore channel into an integrated process chain, as shown in Fig. 1.

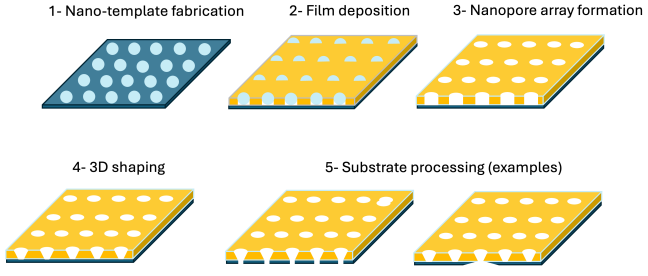

Fig. 1 Illustration of the hybrid fabrication process

2. Controllable Formation of Large-scale Solid-state Nanopore Array

Polystyrene (PS) nanospheres were dispersed onto the silicon wafer by spin coating and form a monolayer distribution. Then, plasma etching can be used to shrink the PS nanospheres to precisely control the nanosphere size and the interval. Afterwards, physical vapor deposition (PVD) is used to deposit a layer or multi-layer of selected materials. Then, by thermal processing, 3D geometry (including size and shape) of nanopores can be changed in a controllable manner. Finally, by etching the substrate in an appropriate way, one or more of nanopores can be exposed as through holes in selected areas.

The monolayer distribution of 100 nm-diameter PS nanospheres was achieved by spin coating as shown in Fig. 2, with controllable densities. The SEM (scanning electron microscope) image in Fig. 2 (a) proves the large area monolayer distribution, actually across a 10 mm× 10 mm area. Fig. 2 (b) indicates a looser distribution with no spheres in contact with each other. In such a condition, nanosphere shrinkage is not necessary as sufficient space exists between nanospheres for material deposition. Fig. 2 (c) shows an extremely sparse distribution where only one nanosphere is in the field of view. Fig. 2 (d) is the AFM (atomic force microscope) detected 3D topography which further verifies the monolayer distribution. It is rare to see large area monolayer distribution of PS nanospheres with diameter below 200 nm from prior literatures.

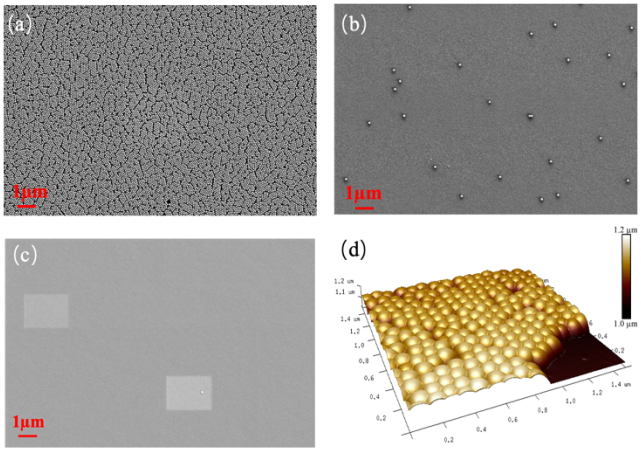

Fig. 2 Monolayer distribution of nanospheres in various densities. (a) SEM image of a large area compact monolayer distribution, (b) SEM image of a looser distribution, (c) SEM image of a single nanosphere, (d) AFM image of 3D topography.

Controlling the size of PS nanospheres is an essential step to set suitable space between nanospheres for subsequent film deposition, meanwhile precisely control the nanopore dimension. Oxygen plasma etching is an effective means to shrink the PS nanospheres. It can be seen from Fig. 3 that the increasing etching time decreased the diameters of nanospheres and the distances between them expanded correspondingly. The average diameters from non-etching to etching 90 s and 120 s were individually calibrated, marking 98.8 ± 1.3 nm, 77.9 ± 2.0 nm, 76.3 ± 2.2 nm, respectively. The correlated dimension tolerances are ± 1.3%, ± 2.6%, ± 2.9%, indicating an enlarged tolerance gradually. Within 120s, it kept within a narrow range thus proved an excellent uniformity maintained during etching. Actually, we did observe a threshold beyond which the nanospheres began to deform and not uniform any more. Experiments by now demonstrated that for 100 nm-diameter nanospheres, the round shape was kept well and uniform in a large scale until 68 nm when some nanospheres began to deform.

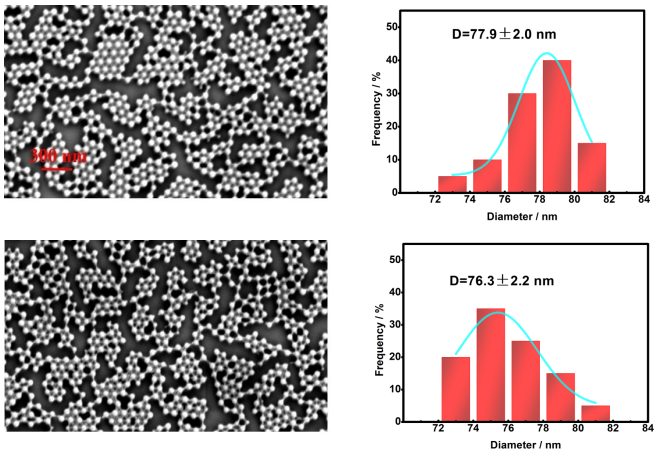

Fig. 3 Oxygen plasma etching of PS nanospheres. Top: etching 90s, bottom: etching 120s.

A variety of materials are applicable for forming the nanopore array membrane, such as SiO_2, Si_3N_4, Al_2O_3, Pt, Ni, Ti, etc. Depending on the PVD accuracy and nanosphere diameter, film thickness can range from several nanometers to hundreds of micrometers. Afterwards, by removing nanospheres, nanopores appeared from where the nanospheres originally existed. The compact or loose distribution of nanopores with perfect boundary and excellent uniformity can be apparently observed via SEM images in Fig. 4, which are all 68 nm in diameter. The chip size is 10 mm ×10 mm, containing about 2.6×10^{10} nanopores in Fig. 4 (a). The density of nanopores can be controlled effectively by regulating the dispersion of nanospheres, denser or looser, directly reflecting the total quantity of nanopores in the chip.

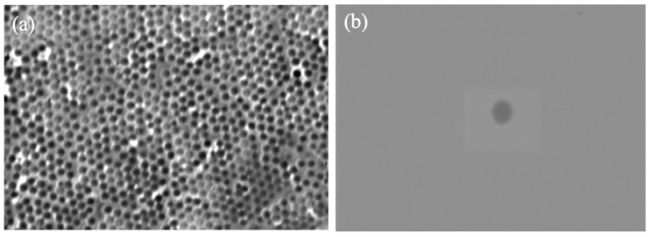

Fig. 4 SEM images of large-scale solid-state nanopore array. The material is SiO_2. (a) Compact nanopore array. (b) A single nanopore.

3. Directed Atomic Migration for 3D Shaping of Nanopores

Nanopore shrinkage stimulated by external energy has been observed by prior research, either by thermal processing or via electron/ion beam irradiation. Although the consensus on the mechanism behind the phenomenon has not been reached, a classic model commonly used by these research is that pores with diameter smaller than the film thickness tend to shrink while pores with diameter larger than the film thickness tend to expand. Most hypotheses

contributed this phenomenon to viscous flow induced by surface tension. However, in our experiments, we observed a totally different phenomenon which was inconsistent with the classic model. When thickness of the nanopore array film was smaller than the diameter of nanopores, such as smaller than radius in our experiments, according to the classic model, nanopores should expand. But we did evidence an inhomogeneous variation of nanopore geometry, indicating the top part expanded while the bottom shrunk, forming a conical nanopore eventually.

To investigate the mechanism and explain this novel phenomenon, DFT simulation based on atomic interaction was performed, which revealed atomic migration from adjacent surface into nanopores and translocate within the nanopore channel. As shown in Fig. 5, a cylindrical nanopore model was built and then put in a simulated thermal field. Four representative locations are pointed out from top to bottom. The distances are measured from the same reference Si atom near the nanopore top entrance (denoted in green in Fig. 5), which were 9.045 Å, 10.395 Å, 16.030 Å and 18.461 Å respectively, deeper toward the nanopore bottom. It was interesting to find that the interaction energy between the SiO_2 molecule and these selected atoms had discrepancies and formed certain rules. After calculation, their interaction energy from the top position to the bottom position are 5799 Kcal/mol, 3983 Kcal/mol, 3623 Kcal/mol and 1422 Kcal/mol respectively. We use this as the indicator to manifest that the top atoms are more active with less energy barrier for interaction while the lower atoms are more restricted. This indirectly reflects that the lower atomic configuration of nanopore channel is more stable than the upper part, forming a gradient of energy potential along the pore channel to drive the atomic flow along certain path. Thus, atoms tend to flow to a lower energy position where should be more stable. This explains why nanopore closed from the bottom first as atoms have the tendency to translocate from the higher part to the lower part. Therefore, we proposed a new mechanism - directed atomic migration to interpret the nanopore shaping.

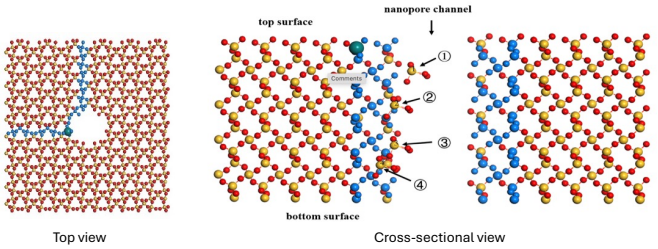

Fig. 5 Illustration of the nanopore channel model.

The proposed mechanism explains why the nanopore seemed larger during experiments, as surface atoms adjacent to the nanopore flowed towards and into the pore and formed a crater around the pore entrance (see Fig. 6). It was observed that the 68 nm-diameter nanopore kept shrinking at 10 mins, 15 mins, 20 mins by thermal processing, and eventually closed around 30 mins. We also found the closure of nanopores across the whole chip. Moreover, it is interesting to find that the pore seemed becoming larger and shallower as in Fig. 6, which proved the inhomogeneous variation along the nanopore channel. Different from previous research that commonly observed a quite regular shrinkage or expansion of nanopores during which nanopore geometry (such as cylindrical) basically kept unchanged, we found a more complex variation of nanopore 3D geometry. The top part of nanopore expanded while the bottom part of nanopore shrunk, thus formed a conical channel, as predicted by our simulation. In addition, nanopore closed at the bottom first, then became shallower and eventually disappeared (with a very shallow dent left as Fig. 6). This is totally different from the direct closure of solid-state nanopores observed in previous research.

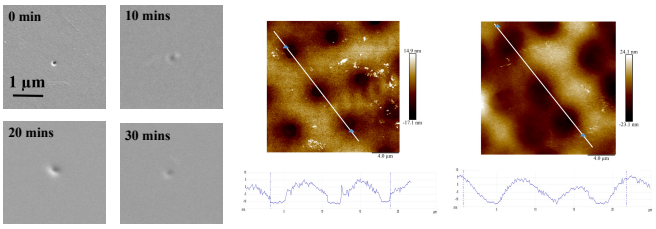

Fig. 6 Atomic migration proved by experiments. Left: Variation of single solid-state nanopore observed via SEM by thermal processing for 0 mins, 10 mins, 20 mins, 30 mins respectively. Right: AFM images of a micropore variation.

To more clearly measure the change of pore geometry, we conducted the 3D shaping experiment on a micropore – a pore with 2 um diameter. From the right part of Fig. 6, AFM detection apparently showed the variation of the cross-sectional profile of the pores. Before processing, the walls of pores are vertical, indicating a cylindrical shape. After processing, the walls became quite smooth, forming a slope extending to the adjacent surface which makes a conical pore geometry. And it can be seen that, the bottom part of the pore became smaller, according well with our mechanism. This provides key evidence to support the atomic and close-to-atomic scale manufacturing (ACSM) [9, 10].

4. Conclusion

An efficient hybrid fabrication method is developed for fabricating large-scale nanopore and micropore array, with excellent uniformity in pore size, shape and density. An innovative directed atomic migration mechanism is proposed to explain the 3D shaping of pore geometry, proved by both simulation and experiments. Disruptive advancements in molecular detection may be enabled, such as parallel DNA sequencing by an integrated chip or selective molecule/cell trapping in high-throughput biomarker detection.

ACKNOWLEDGEMENT

This work is supported by the UCD CEA Seed Fund (R27055), Industrial grant (R27682), partially by the grants from Enterprise Ireland (CF-2022-1986-I), UCD STEM Challenge Fund (R25057) and Science Foundation Ireland (22/RP-2TF/10466 and 21/RC/10295_P2). Authors also expressed acknowledge to Prof. Rao Fu at Dalian University of Technology and Prof. Da Qu at Chongqing University of Technology for supporting the simulation.

REFERENCES

1. Ma Q, Chen L, Gao P, Xia F (2023) Solid-state nanopore/channels meet DNA nanotechnology. Matter 6: 373-396.
2. Chen, Q. & Liu, Z. Fabrication and Applications of Solid-State Nanopores. Sensors 19, 1886 (2019).
3. Wang Y, Deng T, Chen Q, Liang F, Liu Z (2016) Highly efficient shrinkage of inverted pyramid silicon nanopores by plasma enhanced chemical vapore deposition technology. Nanotechnology 27: 254005-2540012.
4. Liu H, Zhou Q, Wang W, Zhang J, Fang F (2023) Solis-State Nanopore Array: Manufacturing and Applications. Small 19: 2205680.
5. Soni G V, Meller A (2007) Progress toward ultrafast DNA sequencing using solid-state nanopores. Clin Chem 53: 1996-2001.
6. Hu R, et al. (2023) Solid-State Quad-Nanopore Array for High-Resolution Single-Molecule Analysis and Discrimination. Adv Mater 35: 10.
7. Chuah K, et al. (2019) Nanopore blockade sensors for ultrasensitive detection of proteins in complex biological samples. Nat Commun 10: 2109.
8. https://store.nanoporetech.com/eu/promethion.html
9. Zhang J, Ducree J (2024) Proposition of Atomic and Close-to-atomic Scale Manufacturing (ACSM). Advances in Manufacturing 12: 1-5.
10. Fang F (2023) On the Three Paradigms of Manufacturing Advancement. Nanomanuf Metrol 6: 35.